CONFERENCE PRE-PRINT

DEUTERIUM INTERACTION WITH LOW-ACTIVATED CHROMIUM-MANGANESE AUSTENITIC STEEL WITH INCREASED CONTENT OF CARBIDE PARTICLES

A.V. GOLUBEVA NRC "Kurchatov institute" Moscow, Russian Federation Email: golubeva_av@nrcki.ru

T.A. SHISHKOVA NRC "Kurchatov institute" Moscow, Russian Federation Email: shishkova tv@nrcki.ru

N.O. STEPANOV NRC "Kurchatov institute" Moscow, Russian Federation

A.E. ALESHIN NRC "Kurchatov institute" Moscow, Russian Federation

A.P. PERSIANOVA NRC "Kurchatov institute" Moscow, Russian Federation

D.A. KOZLOV NRC "Kurchatov institute" Moscow, Russian Federation

D.I. CHERKEZ NRC "Kurchatov institute" Moscow, Russian Federation

I.Yu. LITOVCHENKO ISPMS SB RAS Tomsk, Russian Federation

V.M. CHERNOV VNIINM Moscow, Russian Federation

Abstract

New low-activation austenitic chromium-manganese steel has been recently developed in Russia as a potential structural material for nuclear and fusion reactors. In the present work deuterium interaction with melt No 4 of new steel with increased content of carbide particles was investigated. Deuterium was introduced into steel samples by exposure to D_2 gas at a temperature of 200 °C and a pressure of $5\cdot10^5$ Pa and by 100 eV deuterium plasma irradiation at 200 °C with fluence of up to 10^{25} D/m². Deuterium retention in the new steel was investigated using thermal desorption method. Deuterium permeation into the new steel was studied in a temperature range of 150-380 °C and a deuterium pressure range of $10^3-5\cdot10^4$ Pa. The temperature dependences of deuterium diffusivity and permeability of the new steel were obtained.

1. INTRODUCTION

In industrial fusion facilities, the first wall will be by irradiated with fusion neutrons for 10–20 years. This will result in activation of wall materials and damage level of structural materials of up to 50 dpa [1]. The requirement of low activation of structural materials is important for safety. The austenitic steel SS316L-IG

[Right hand page running head is the paper number in Times New Roman 8 point bold capitals, centred]

used at ITER is acceptable only for the experimental reactor, because the activity induced by neutrons with thermonuclear energies will exceed limits acceptable for personal for more than thousand years after. Until recently, when designing fusion reactor vessels, reduced activation ferritic-marteneitic (RAFM) steels were the only alternative materials to nickel austenitic steels. RAFM steels indeed have undeniable advantages, such as relatively quick decay of induced activity, good thermomechanical properties, absence of helium swelling up to a damage level of 100 dpa. The disadvantages of RAMS are the growth of ductile-to-brittle transition temperature under the action of neutron irradiation and magnetic properties. High-activation nickel austenitic steels like SS316L-IG are free from both of these disadvantages. It would be desirable to create materials that combine advantages of austenitic nickel steels and RAFM steels and do not have their disadvantages.

An idea of creating low activation austenitic steels using manganese instead of nickel was formulated tens of years ago. In the last quarter of 20th century, steels based on Fe-12Cr-(20-25)Mn-0,25C [2-4] with additives of V, W, Ti, B, P, and variants of steel with close compositions [5-7] were developed in several countries. The problem in creating such steels consisted in their phase instability after being irradiated and/or subjected to longtime high-temperature aging [5, 8, 9] leading to a decrease in ductility and embrittlement. Due to this problem, as well as the fact of successful development of RAFM steels, work on the creation of low-level activated austenitic steels was suspended everywhere.

Several years ago, work in this field was resumed in Russia. New low-activation austenitic chromiummanganese steels (LAAS) have been created, being patented in 2024 [10]. The obtained strength and plastic properties of new low-activation austenitic steel and its thermal stability under conditions of prolonged (up to 500 h) aging at 700 °C allows considering these steels as promising low-activation structural materials for fusion and hybrid reactors [11-13].

The interaction of hydrogen isotopes with low-activation austenitic chromium-manganese steels has never been studied before. Meanwhile, in terms of radiation safety, it is very important to know the parameters of tritium retention and transport in material proposed as a structural material for fusion facilities. Due to the complexity of organizing experiments with radioactive tritium, under the laboratory conditions, its interaction with materials is often modelled by means of performing experiments with deuterium. This approach is also used in this work.

The goal of this work is to obtain parameters of deuterium interaction with new low-activated austenitic chromium-manganese steel.

The object of study is the LAAS melt No. 4 (LAAS #4).

2. MATERIAL AND SAMPLES

The composition of LAAS melt No. 4 is presented in the Table 1. Melting of 10 kg of steel was performed in a vacuum induction furnace. After melting, the steel was homogenized at 1100 °C for 4 hours and hammered at 1100 °C, followed by its hot rolling (at 1100 °C) into sheets. Next, the guenched state was obtained (after the exposure at 1100 °C for 1 hour followed by air cooling). Cold-rolled samples were obtained from the quenched samples. Studies of the samples microstructure show the presence of complex-doped carbides in the material: MC with a typical particle size of 50-100 nm and M₂₃C₆ with a particle size of 100-150 nm. In novel steel of melt No. 4, the content of carbide particles was increased, as compared to previously studied steels [2-9]. According to the modeling performed using the JMatPro code, the equilibrium contents of MC and M23C6 carbide particles are less than 0.5 and 5 atm. %, respectively. According to results of microstructure investigations for the samples considered in this work, the content of MC particles is less than 0.2-0.3 atm. %, and the content of $M_{23}C_6$ carbides was assumed to be in the range of 2-3 atm. %. Plates with a thickness of 10 mm and thin plates with a thickness of 1.2 mm were obtained from cold-rolled samples using electric discharge sawing. Several double-sides flanges DN16CF were turned out of a 10-mm-thick plate. In experiments on studying permeability, the central areas of flanges with diameters of 16 mm and thicknesses of ~ 0.25 mm acted as membranes. For experiments on studying retention, 10×10 mm samples were cut from the 1.3-mm-thick sheet using electric discharge sawing. These samples were mechanically polished from both sides to high finish, and as a result their thickness being reduced to 1 mm. Finally the samples were washed in acetone and heated in vacuum for 2 hours at a temperature of 773 K.

TABLE 1. COMPOSITION OF LAAS MELT NO. 4, WT. %

Cr	Mn	Ni	Cu	W	V	Ti	Nb	Mo	Со	Al	Si	S	P	С	В
11,3	22,4	0,015	<0,05	1,08	0,2	0,17	0,01	0,01	0,02	0,04	0,47	0,006	<0,01	0.3	0,004

3. EXPERIMENTAL

3.1. Permeation

Gas-driven permeation of hydrogen isotopes though LAAS were investigated at the GDP facility [14]. The membrane separates two ultra-high vacuum volumes with a residual pressure $\sim 10^{-7}$ Pa. The membrane is surrounded with heater, and the membrane temperature is measured using chromel-alumel thermocouple. The first volume could be filled with deuterium or hydrogen gas at a pressure in the range of $5 \cdot 10^2 - 10^5$ Pa. The differential method was used for studying the deuterium permeation at constant pump-down of the second volume, into which the permeating flow incomes. The second volume is equipped with quadrupole mass-spectrometer (QMS), which records partial pressures of a number of gases, including H_2 , HD, D_2 , HDO and D_2O . In present work, contribution of desorption as water molecules in the permeating deuterium flow was less than 1 % and, therefore, it was not taken into account. At constant pump-down, the increment of partial pressure of some gas in the chamber is proportional to the inflow of this gas into the chamber. Using the calibration system based on the diaphragm with known size and the baratron-type pressure gauge, the QMS calibration was performed. As a result, H_2 and H_2 partial pressures determined by QMS could be recalculated into flows of corresponding molecules from the outlet membrane surface. The average between the calibration coefficients for H_2 and H_2 was taken as a calibration coefficient for H_2 and H_2 and H_3 was taken as a calibration coefficient for H_3 molecules.

3.2. Exposure to deuterium gas

The samples were exposed to D_2 gas in the saturation module. The module is 0.04 l vacuum vessel, which can be pumped down to a pressure of 10^{-5} Pa and filled with deuterium at a pressure of up to 10 atmospheres. The saturation module is surrounded by external heater, and the temperature inside can be maintained in the range up to 700 °C for a long time. The temperature inside the module is controlled using the chromel-alumel thermocouple; the gas pressure in the module was measured by the baratron-type sensor. In the present work, samples were exposed to D_2 gas at a pressure $5 \cdot 10^5$ Pa and a temperature of 200°C for 25 or 100 hours.

3.3. Plasma irradiation

Irradiation of the samples by deuterium plasma was performed at the PIM stand [15] equipped with the source of low-temperature plasma with the electron temperature of $Te \sim 3-5$ eV and ion temperature of $Te \sim 0.4$ eV. At the PIM stand the ratio of hydrogen ion contents in the plasma is $H_3^+:H_2^+:H^+=7:2:1$. The flow of neutral atoms onto the sample surface is up to 30% of the ion flow. Five samples were mounted with the help of a molybdenum mask on the copper sample holder 35 mm in diameter. Due to a large (150 mm) size of homogeneous plasma zone, the samples were irradiated under identical conditions. The bias voltage applied to the sample holder determines the energy of ions irradiating the surface. The heater is mounted at the sample holder side opposite to the plasma. During irradiation, the temperature is measured using the chromel-alumel thermocouple attached to the sample holder between samples and shielded from plasma by the mask. In the present work, the samples were irradiated by 100-eV deuterium plasma with a flux of 2×10^{20} at. $D/(s\cdot m^2)$ at 200 °C up to an irradiation dose of $5\cdot10^{24}$ D/m^2 .

3.4. Samples storage

After exposing the samples to deuterium gas, they were stored in air under normal conditions. The storage time of the samples exposed to gas flow was 1-43 days. After irradiation by deuterium plasma, most of the samples were stored at high vacuum conditions at a pressure of 10^{-6} Pa. The storage time ranged from 1 to 61 days.

3.4. Deuterium retention

The deuterium retention was investigated at the UHV stand using thermal desorption spectroscopy (TDS). The steel samples under investigation were heated up to 1223 K in vacuum in a quartz bulb using external halogen lamps with a constant heating rate of 0.5 K/s. In the course of heating, partial pressures of several of gases, including H₂, HD, D₂, HDO and D₂O, were measured by QMS. Each sample was twice subjected to the thermal desorption procedure: during the first heating, deuterium was removed from the sample; during the second heating, the background signal of deuterium was recorded, which corresponded to deuterium desorbed in the

course of heating from the elements surrounding the sample. Further in the work, thermal desorption spectra are presented, which were obtained after subtracting the background signals recorded during the second heating. The QMS calibration coefficients for H_2 , HD and D_2 flows were found similarly to those used in permeation measurements described above. Deuterium was desorbed from LAAS samples predominantly in the form of D_2 molecules, and also in the form of HD, HDO, and HD0 molecules. Calibration coefficients for HD and HD2 molecules were used to estimate deuterium desorbing in the composition of HDO and HD2 molecules, respectively. In publications, similar assumptions are often made when calculating the deuterium yield in the composition of heavy water [16, 17]. Further, when considering the HDS1 spectra, we will discuss the amount of deuterium that can be accurately determined: deuterium desorbed in the form of HDS2 and HD3 molecules. This results in underestimation of the integral deuterium retention by no more than 6%, and it does not have a fundamental effect on the results obtained and conclusions drawn.

4. RESULTS AND DISCUSSION

Since the interaction of hydrogen with low activation chromium manganese steels had not been studied before, at the beginning of work we could only make one assumption that no hydrides will form in the bulk of LAAS, since it does not include hydride-forming elements. In this case, hydrogen in metal can be in dissolved state (in interstices of crystal lattice) or it can be captured in some trap, which is a state with the higher binding energy than that in dissolved state. Almost any defect in the crystal lattice can act as a trap for hydrogen in metal.

4.1. Permeation

According to popular model [18], the first stage of the process of hydrogen permeation into metal is the adsorption of molecules and their dissociation at the inlet membrane surface. The chemosorbed atoms can overcome the entrance energy barrier, diffuse though the bulk and reach opposite membrane surface. After recombination of hydrogen atoms at outlet, molecules become desorbed, forming the permeating flow.

In permeation measurements, two membranes were used. Membrane No. 1 without coatings was installed first. In experiments with this membrane, the steady-state permeating flow was not obtained. After injection of D_2 gas above the inlet membrane surface, the permeating flow appeared above the inlet membrane surface; it at first increased, then reached its maximum, after which decreased. Such dynamics is typical of the cases when one or both membrane surfaces are oxidized in the course of the experiment. To prevent membrane surface from modification during the experiments, both sides of the second membrane were pre-cleaned from oxides by means of irradiating them with Ar plasma and coated with 100-nm-thick palladium deposited using magnetron sputtering. In contrast to the case of using uncoated membrane No. 1, when using Pd-coated membrane No. 2, the permeating flow always became steady-state.

Time dependences of deuterium fluxes permeating through two membranes at a pressure of $5 \cdot 10^3$ Pa are shown in Fig. 1. In experiments with Pd-coated membrane No. 2, permeating flux reached its maximum several times faster and was an order of magnitude higher than that in the case of uncoated membrane No. 1.

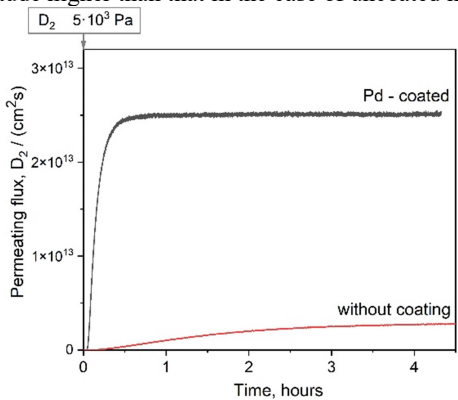


FIG. 1. Time dependences of deuterium fluxes permeating through uncoated membrane No. 1 and Pd-coated membrane No. 2 at 310°C and D_2 pressure of $5 \cdot 10^3$ Pa.

So, the presence of natural oxides on LAAS surfaces considerably slows down deuterium transport and reduces permeating flux. This result is not surprising since oxide films on the surfaces of a number of metals have barrier properties [19, 20].

Palladium crystal lattice has the FCC structure and is characterized by high hydrogen solubility. In the temperature range considered in the present work (150–380 °C), the hydrogen diffusion coefficient in palladium is 3 orders of magnitude higher than that in the SS316 nickel austenitic steel [21].

One of the reasons for the faster establishing of stationary regime after removing natural oxides and applying palladium coating on both sides of the membrane is the absence of oxides and preventing the sample surface from oxidation. Also Pd atoms serve as activation centres where deuterium molecules dissociate into atoms, thus accelerating deuterium permeation into the bulk.

The dependences of stationary permeating fluxes on deuterium pressure above the inlet surface of Pd-coated membrane were close to square root dependence (see FIG. 2), indicating diffusion-limited regime (DLR) of permeation, during which the processes at surface proceed considerably faster than diffusion through the bulk.

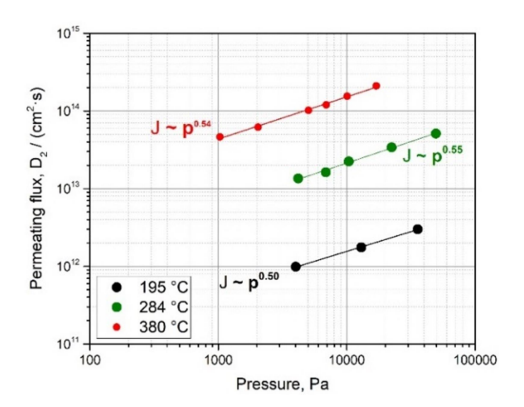


FIG. 2. Dependences of deuterium steady-state flux permeating through Pd-coated membrane No. 2 on D_2 pressure above the inlet membrane surface at fixed temperatures

In this regime, hydrogen diffusion coefficient D, solubility S and permeability P=SD can be rather easily determined using the expression for time dependence of the permeating flux [22]:

$$J_{DLR} = \frac{DS\sqrt{p}}{L} (1 + 2\sum_{n=1}^{\infty} (-1)^n \exp(-\frac{D\pi^2 n^2}{L^2}))$$
 (1)

Coefficients of deuterium diffusion and permeation through LAAS melt No 4 are shown in FIG. 3 along with the corresponding data for other main candidates for fusion structural materials found in publications: austenitic nickel steels and RAFMS. Deuterium diffusivity in LAAS is close to that in nickel steels of the 300th series and is by more than order of magnitude lower than that in RAFM steels. Deuterium permeability through LAAS is several times higher than that through usual nickel austenitic steels and lower than that through the RAFMS steels.

In a temperature range of 150–380 °C, the following temperature dependences were obtained for transport characteristics of deuterium in LAAS:

$$D(T) [m2/s] = 3.2 \cdot 10-6 exp(-58000/RT)$$
 (2)

$$P(T) [mol/(m \cdot s \cdot Pa^{1/2})] = 6.9 \cdot 10^{-6} \exp(-62600/RT)$$
(3)

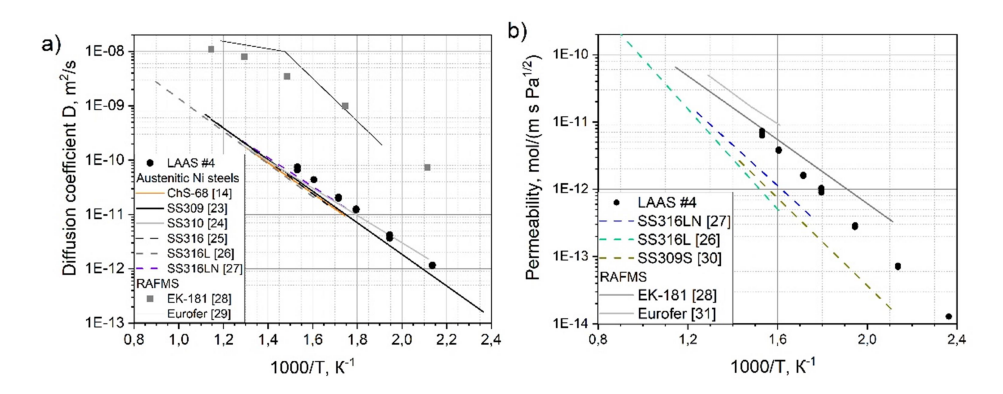


FIG. 3. Temperature dependences of deuterium (a) diffusion and (b) permeation through LAAS, melt No 4.

4.2. Deuterium retention

The TDS spectra of LAAS samples exposed to D₂ gas at 200 °C are shown in FIG. 4.a. On the TDS spectra of exposed-to-gas samples, one broad peak is seen, possibly consisting of several peaks. TDS measurements were performed with different time delays after exposure in gas, in order to find out how deuterium escapes from the LAAS samples with time. The shapes of TDS spectra were reproducible. Total deuterium retention in sample as a function of storage time before measuring the TDS spectra is shown in FIG 4.b. For comparison, the data for the Russian reduced activation ferritic-martensitic steel EK-181, analysed under the same conditions, are also given in FIG 4. The LAAS samples exposed to deuterium gas during 25 hours capture the same amount of deuterium as the Ek-181 steel. However, due to quick diffusion, 25 hours should be enough to reach saturation of the EK-181 samples with deuterium, while it is not the case for the LAAS where diffusion is slower. At exposure time of 100 h, deuterium retention in the LAAS samples is 3,5 times higher than in Ni austenitic steel and 6 times higher than that in Ek-181 samples.

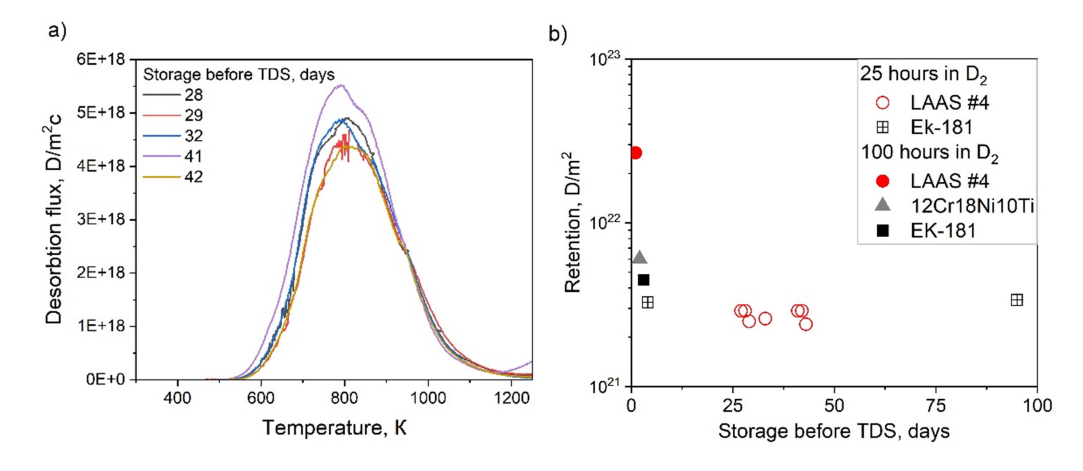


FIG. 4. Deuterium retention in LAAS melt No. 4, exposed to D_2 gas at 200 °C and pressure of $5 \cdot 10^5$ Pa and stored at normal conditions: a) TDS spectra at exposure time 25 hours b) total retention after 25 and 100 hours of exposure in D_2

Retention of deuterium in plasma-irradiated samples is illustrated in FIG. 5. In contrast to the case of samples exposed to D₂ gas, the TDS spectra of plasma-irradiated LAAS samples consist of two peaks (FIG 5.a). Total retention in the LAAS samples (FIG 5.b) is compared with the corresponding data for the 12Cr18Ni10Ti austenitic steel (Russian analog of the SS316 steel) and the EK-181 RAFM steel, irradiated under the same conditions. Deuterium retention in the LAAS samples is 3 times higher than that in the 12Cr18Ni10Ti steel and more than an order of magnitude higher than in the EK-181 steel.

Thus, LAAS has considerably higher retention capacity relative to hydrogen than the EK-181 steel and several times higher capturing capacity than the austenitic steels of the 300th grade. An increased content of carbide particles is definitely one of the reasons for high retention, since such particles strongly capture hydrogen [32,

33]. It is still a question whether other factors, in particular high Mn concentration, can contribute to hydrogen retention.

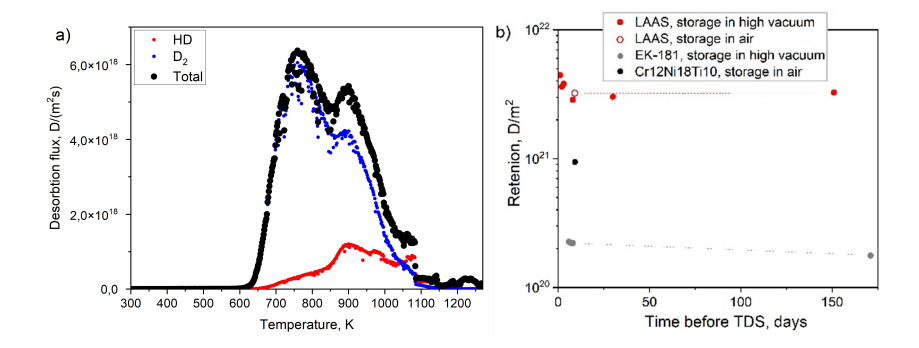


FIG. 5. Deuterium retention in LAAS irradiated with 100-eV-energy D-plasma at 200 °C and up to a doze of 5·10²⁵ D/m²: a) TDS spectrum, b) total retention as compared with 12Cr18Ni10Ti nickel austenitic steel and EK-181 RAFM steel irradiated under the same conditions

5. CONCLUSIONS

The deuterium interaction with new Russian low-activation chromium-manganese austenitic steel with increased content of carbide particles was investigated.

The temperature dependences of diffusivity and permeability through the new steel were obtained in a temperature range of 150–380 °C. Deuterium diffusivity in LAAS is close to that in nickel steels of the 300th series and more than order of magnitude lower than that in RAFM steels. Deuterium permeability through LAAS is several times higher than that through usual nickel austenitic steels and lower than that through Ek-181 steel. At 350 °C, natural oxides on the surfaces of 0.25-mm-thick LAAS membrane reduce permeating deuterium flux by an order of magnitude.

Deuterium retention in LAAS was investigated after exposing samples to D_2 gas at a temperature of 200 °C and a pressure of $5\cdot10^5$ Pa, as well as after irradiating them with D-plasma at 200 °C up to a doze of 10^{25} D/m². LAAS captures considerably higher amounts of deuterium as compared with RAFM steel the EK-181 and the 12Cr18Ni10Ti austenitic steel. An increased content of carbide particles is supposed to be among the reasons for high retention.

FUNDING

The work was supported by the National Research Center "Kurchatov Institute" under the State Assignment.

REFERENCES

- N. ASAKURA et al., Recent progress of plasma exhaust concepts and divertor designs for tokamak DEMO reactors, Nucl. Mater. & Energy, 2023, Vol. 35, 101446
- [2] KLUEH R.L. et al., Reduced Activation Materials for Fusion Reactors, Philadelphia, PA, USA: ASTM, 1990.
- [3] KLUEH R.L. et al. Tensile and microstructural behavior of solute-modified manganese-stabilized austenitic steels, Materials Science and Engineering: A, 1990, Vol. 127., p. 17–31.
- [4] KLUEH R.L. Tensile behavior of irradiated manganese-stabilized stainless steels, J. Nucl. Mater., 1996, Vol. 233–237, p. 197–201.
- [5] DEMINA E.V. et al., Radiation Creep and Phase Instability of Low-Activation Austenitic Steel 12 Cr–20 Mn–W under Neutron Irradiation in the FFTF Fast Reactor, Inorganic Materials: Appl. Research, 2011, Vol. 2, p. 457–460
- [6] ONOZUKA M. et al, Low-activation Mn–Cr austenitic stainless steel with further reduced content of long-lived radioactive elements, J. Nucl. Mater., 1998, Vol. 255, p.. P. 128–138.
- [7] SUZUKI Y. et al., Low activation austenitic Mn-steel for in-vessel fusion materials, J. Nucl. Mater., 1998, Vol. 258–263, p. 1687–1693.

[8] ABE F. et al., Discontinuous precipitation of σ-phase during recrystallization in cold rolled Fe-10Cr-30Mn austenite, Mater. Sci. Technol., 1988, Vol. 4, p. 885-893.

[Right hand page running head is the paper number in Times New Roman 8 point bold capitals, centred]

- [9] KLUEH R.L. et al., Manganese as an Austenite Stabilizer in Fe-Cr-Mn-C Steels, Mater. Science & Engineering: A, 1988, Vol. 102, p. 115-124.
- [10] LITOVCHENKO I.Yu. et al., Low activation chromium manganese austenitic steel, Малоактивируемая хромомарганцевая аустенитная сталь, Patent RU 2821535 C1, Russian Federation, 2024
- [11] LITOVCHENKO I. et al., Microstructure Features and Mechanical Properties of Modified Low-Activation Austenitic Steel in the Temperature Range of 20 to 750 °C, Metals, 2023, Vol. 13 2015
- [12] LITOVCHENKO I.Yu. et al., Effect of aging at 700 °C on the microstructure, phase transformations, and mechanical properties of low-activation austenitic steel, Materialia, 2025, Vol. 39, 102335
- [13] LITOVCHENKO I.Yu. et al., Microstructure and mechanical properties of Y-modified low-activation austenitic steel after aging, Russian Physics Journal, 2025, 67 (5) p. 2041-2048
- [14] A.V. GOLUBEVA et al., A GDP Facility for Studying the Permeability of Membranes Interacting with Gaseous Hydrogen, Instruments and Experimental Techniques, 2022, Vol. 65, No. 5, pp. 837–848
- [15] A.V. GOLUBEVA et al., "A Facility for Permeation Measurements under Plasma Irradiation" // Instruments and experimental techniques, 2017, Vol. 60 No. 6, p. 843-852
- [16] KRAT S.A. et al., Comparison of deuterium retention in tungsten films of various thickness, // Nuclear Physics and Engineering, 2024. Vol.15(3). C.218-223 (In Russian)
- [17] ZHAO M. et al., Deuterium retention behavior of pure and Y2O3-doped tungsten investigated by nuclear reaction analysis and thermal desorption spectroscopy, Nucl. Mater. & Energy, 2018, Vol.15, p. 32-42
- [18] M.A. PICK et all, A model for atomic hydrogen-metal interactions application to recycling, recombination and permeation, J. Nucl. Mater., 1985, Vol.131, p. 208 - 220
- [19] TANABE T. et al., Hydrogen transport in stainless steels, J. Nucl. Mater., 1984, Vol. 123, p. 1568–1572.
- [20] LYU Y.-M. et al., Effects of oxidation on the deuterium permeation behavior of the SIMP steel, International Journal of Hydrogen Energy, 2019, Vol. 44, p. 18265-18271
- [21] Hydrogen diffusion in metals, data compilation, edited by D.J. Fisher, Trans tech publications, 2014
- [22] A.A. Pisarev et al., Permeability of hydrogen through metals, Moscow, 2008, MEPhI (In Russian)
- [23] Kass W. J., Andrzejewski W. J.: AEC Rep. Sc-DR-72-0136, 1972
- [24] QUICK N. R. et al, Permeation and diffusion of hydrogen and deuterium in 310 stainless steel, 472 K to 779 K, Metallurgical Transactions A. 1979. V.10. №1. P. 67 –70
- [25] REITER F. et al, Interaction of Hydrogen Isotopes with Stainless Steel 316 L, Fus. Techn., 1985, Vol. 8, p. 2344-2351
- [26] LEE S. K. et al, Deuterium transport and isotope effects in type 316L stainless steel at high temperatures for nuclear fusion and nuclear hydrogen technology applications, Current Applied Physics, 2014, Vol. 14, p. 1385–1388.
- [27] HOUBEN A. et al., Comparison of the hydrogen permeation through fusion relevant steels and the influence of oxidized and rough surfaces, Nucl. Mater. Energy, 2019, Vol. 19, p. 55-58.
- [28] I.V. DANILOV et. al, Facility for studies of structural materials permeability to hydrogen isotopes, Questions of atomic sc. & techn, Ser. Fusion, 2014, Vol. 37, I. 2, p. 38-44 (in Russian)
- [29] ZE CHEN et al., Deuterium transport and retention properties of representative fusion blanket structural materials, J. Nicl. Mater, 2021, Vol. 549, 152904
- [30] SWANSIGER W.A. et. al, Tritium and deuterium permeation in stainless steels: influence of thin oxide films, J. Nucl. Mater., 1979, Vol 85-86, p.335-339.
- [31] D. LEVCHUK et al., Deuterium permeation through Eurofer and a-alumina coated Eurofer, J. Nucl. Mater., 2004, Vol. 328, pp. 103-106
- [32] V.KH. ALIMOV, Exposure of reduced activation ferritic/martensitic steels to deuterium plasma. Review of data on surface modification, diffusion and accumulation of deuterium, Journal of Surface Investigation, 2025, vol. 19, Issue 5,
- [33] Mizuno M. et al. Determination of hydrogen concentration in austenitic stainless steels by thermal desorption spectroscopy //Material Transactions, JIM. – 1994. – V. 35. – №10. P. 703-707.